AMERICAN SOCIETY FOR MICROBIOLOGY | Applied and Environmental Microbiology®

BIOTECHNOLOGY

Engineering Pseudochelin Production in *Myxococcus xanthus*

Juliane Korp,[a,b] Lea Winand,[a] Angela Sester,[a,b] Markus Nett[a]

[a]Department of Biochemical and Chemical Engineering, Laboratory of Technical Biology, TU Dortmund University, Dortmund, Germany

[b]Leibniz Institute for Natural Product Research and Infection Biology, Hans Knöll Institute, Jena, Germany

ABSTRACT Myxobacteria utilize the catechol natural products myxochelin A and B in order to maintain their iron homeostasis. Recently, the production of these siderophores, along with a new myxochelin derivative named pseudochelin A, was reported for the marine bacterium *Pseudoalteromonas piscicida* S2040. The latter derivative features a characteristic imidazoline moiety, which was proposed to originate from an intramolecular condensation reaction of the *β*-aminoethyl amide group in myxochelin B. To identify the enzyme catalyzing this conversion, we compared the myxochelin regulons of two myxobacterial strains that produce solely myxochelin A and B with those of *P. piscicida* S2040. This approach revealed a gene exclusive to the myxochelin regulon in *P. piscicida* S2040, coding for an enzyme of the amidohydrolase superfamily. To prove that this enzyme is indeed responsible for the postulated conversion, the reaction was reconstituted *in vitro* using a hexahistidine-tagged recombinant protein made in *Escherichia coli*, with myxochelin B as the substrate. To test the production of pseudochelin A under *in vivo* conditions, the amidohydrolase gene was cloned into the myxobacterial plasmid pZJY156 and placed under the control of a copper-inducible promoter. The resulting vector was introduced into the myxobacterium *Myxococcus xanthus* DSM 16526, a native producer of myxochelin A and B. Following induction with copper, the myxobacterial expression strain was found to synthesize small quantities of pseudochelin A. Replacement of the copper-inducible promoter with the constitutive *pilA* promoter led to increased production levels in *M. xanthus*, which facilitated the isolation and subsequent structural verification of the heterologously produced compound.

IMPORTANCE In this study, an enzyme for imidazoline formation in pseudochelin biosynthesis was identified. Evidence for the involvement of this enzyme in the postulated reaction was obtained after *in vitro* reconstitution. Furthermore, the function of this enzyme was demonstrated *in vivo* by transferring the corresponding gene into the bacterium *Myxococcus xanthus*, which thereby became a producer of pseudochelin A. In addition to clarifying the molecular basis of imidazoline formation in siderophore biosynthesis, we describe the heterologous expression of a gene in a myxobacterium without chromosomal integration. Due to its metabolic proficiency, *M. xanthus* represents an interesting alternative to established host systems for the reconstitution and manipulation of biosynthetic pathways. Since the plasmid used in this study is easily adaptable for the expression of other enzymes as well, we expand the conventional expression strategy for myxobacteria, which is based on the integration of biosynthetic genes into the host genome.

KEYWORDS *Myxococcus xanthus*, pseudochelin, myxochelin, expression plasmid, imidazoline synthase, biosynthesis, myxobacteria

Iron is indispensable for microbial viability. It acts as a component of several enzymes and enzymatic complexes and hence is essentially involved in various biological processes, such as respiration, amino acid synthesis, oxygen transport, and DNA

Received 23 July 2018 **Accepted** 1 September 2018

Accepted manuscript posted online 14 September 2018

Citation Korp J, Winand L, Sester A, Nett M. 2018. Engineering pseudochelin production in *Myxococcus xanthus*. Appl Environ Microbiol 84:e01789-18. https://doi.org/10.1128/AEM.01789-18.

Editor Isaac Cann, University of Illinois at Urbana-Champaign

Address correspondence to Markus Nett, markus.nett@tu-dortmund.de.

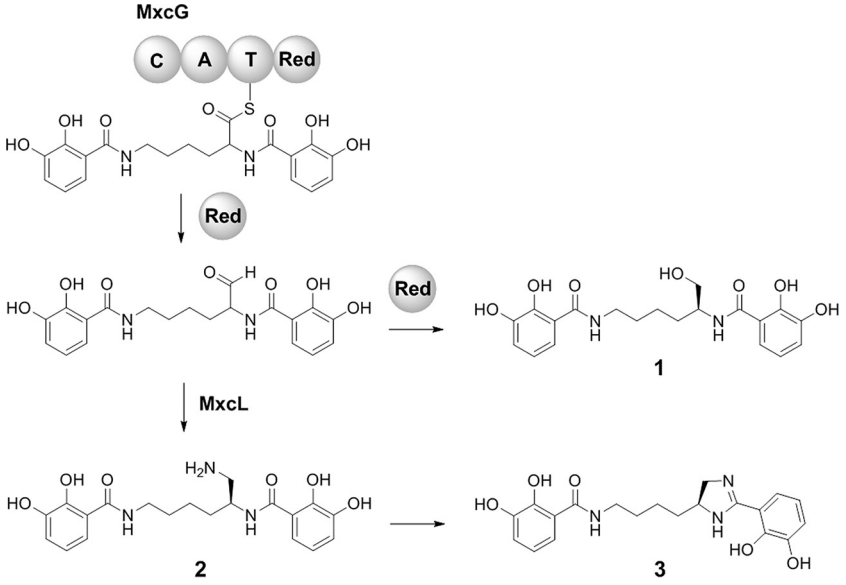

FIG 1 Late steps in the biosynthesis of myxochelin A (compound 1) and myxochelin B (compound 2), as well as pseudochelin A (compound 3). The NRPS MxcG consists of an N-terminal condensation (C) domain, followed by an adenylation (A), a thiolation (T), and a C-terminal reductase (Red) domain.

biosynthesis. Although iron is abundant in nature, the metal exists predominantly in an insoluble and biologically inaccessible ferric (Fe^{3+}) form under aerobic conditions and at physiological pH. To facilitate the uptake of ferric iron, many bacteria resort to low-molecular-weight iron-chelating compounds, so-called siderophores. These molecules are secreted from the cells in order to solubilize and to capture ferric iron. Subsequently, the ferric iron-siderophore complex is actively transported back into the bacterial cytoplasm and the coordinated ion is released by either reductive or hydrolytic mechanisms (1–3).

Myxobacteria are Gram-negative soil inhabitants. They possess an unusually complex life cycle, which involves differentiation from individual cells into multicellular fruiting bodies under starvation conditions, accompanied by sophisticated social behavior (4–6). In recent years, myxobacteria have gained increasing attention due to their enormous potential as producers of secondary metabolites with antifungal, antibacterial, and cytotoxic activities (7–9). To maintain their iron homeostasis, many myxobacteria produce catechol siderophores, such as the myxochelins (10–13) or the structurally related hyalachelins (14). Although the myxochelins are generally regarded as myxobacterial siderophores, they were occasionally also described for other bacteria. Examples include the actinomycete *Nonomuraea pusilla* (15) and the *Chloroflexi* bacterium *Herpetosiphon aurantiacus* (16).

The biosynthesis of myxochelins has been thoroughly explored both on the genetic level (17) and on the biochemical level (11, 18–20). Briefly, a nonribosomal peptide synthetase (NRPS) termed MxcG links two 2,3-dihydroxybenzoate (DHBA) units with the amino groups of L-lysine. The resulting thioester intermediate is reduced to an aldehyde by the reductase domain of MxcG and thereby is released from the enzyme complex (Fig. 1). A subsequent reduction reaction forms myxochelin A (compound 1), whereas the transamination of the aldehyde, catalyzed by an aminotransferase (MxcL), leads to myxochelin B (compound 2). Recently, a novel myxochelin derivative termed pseudochelin A (compound 3) was isolated from the marine bacterium *Pseudoalteromonas piscicida* S2040 (21). Pseudochelin A features a characteristic 4,5-dihydroimidazole moiety, putatively emerging from an intramolecular cyclization reaction of myxochelin B (Fig. 1). In this study, the genetic basis of this biosynthetic reaction was determined by comparative genomics and heterologous reconstitution. Among others, *Myxococcus*

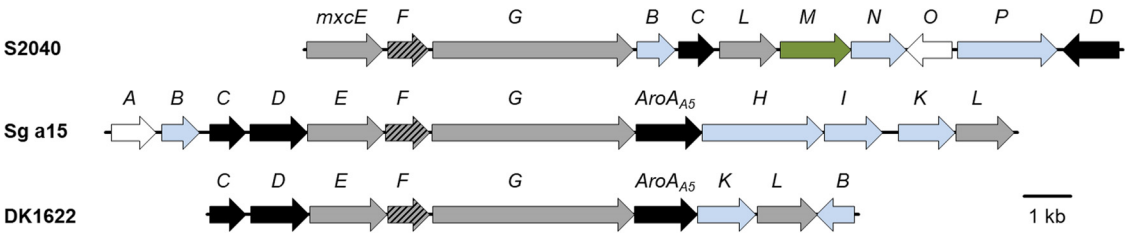

FIG 2 Organization of the myxochelin regulons in *P. piscicida* S2040, *S. aurantiaca* Sg a15, and *M. xanthus* DK 1622. Genes involved in DHBA and myxochelin biosynthesis are highlighted in black and gray, respectively. The hatched *mxcF* is required during both processes. Transport genes are depicted in blue. Regulatory and accessory genes are marked in white. The candidate gene for pseudochelin formation is highlighted in green.

xanthus strains that are able to produce pseudochelin A were engineered. For this, myxobacterial expression vectors were created.

RESULTS

Organization of the myxochelin regulon in *P. piscicida* S2040. The myxobacteria *Stigmatella aurantiaca* Sg a15 and *M. xanthus* DK 1622 are known producers of myxochelin A and B (12, 17). Furthermore, the myxochelin regulon of *S. aurantiaca* Sg a15 has already been comprehensively analyzed (17); it comprises 12 genes, of which 3 (*mxcE*, *mxcF*, and *mxcG*) were shown previously to be sufficient for the assembly of myxochelin A from DHBA and L-lysine, while the aminotransferase gene *mxcL* is further needed for myxochelin B biosynthesis (11, 18). MxcF represents a bifunctional enzyme. It features an aryl carrier protein domain for tethering the activated DHBA building block during myxochelin assembly. Beyond that, its isochorismatase domain is involved in the conversion of chorismate into DHBA in conjunction with two other enzymes, MxcC and MxcD (17). The corresponding set of six core biosynthesis genes (*mxcC* to *mxcG* and *mxcL*) is also present in the myxochelin regulon of *M. xanthus* DK 1622, which consists of nine genes in total. Using the nucleotide sequences of the conserved biosynthesis genes as probes, a putative myxochelin locus was located in the genome of the pseudochelin producer *P. piscicida* S2040 by homology-driven alignment (Fig. 2). The corresponding regulon covers a contiguous DNA sequence of about 17 kb and includes 11 genes (GenBank accession numbers TW75_RS20420 to TW75_RS20470), which were renamed in this study according to the nomenclature used in previous publications (17–19). Seven of these genes have homologs in the myxochelin regulons of *S. aurantiaca* Sg a15 and *M. xanthus* DK 1622 (Table 1). In addition to the six myxochelin biosynthesis genes, *P. piscicida* S2040 contains a homolog of *mxcB*, coding for a NADPH-dependent ferric siderophore reductase. The latter removes the metal from an iron-bound myxochelin following its cellular uptake. Four genes (*mxcM*, *mxcN*,

TABLE 1 Distribution and putative function of myxochelin biosynthesis genes

Gene	Putative function	*S. aurantiaca* Sg a15 vs *P. piscicida* S2040[a]		*M. xanthus* DK 1622 vs *P. piscicida* S2040[a]	
		% Id	% Qc	% Id	% Qc
mxcE	2,3-DHBA-AMP ligase	51	98	50	98
mxcF	Isochorismatase/aryl carrier protein	44	97	44	97
mxcG	Nonribosomal peptide synthetase	37	98	38	99
mxcB	Ferric siderophore reductase	37	90	36	86
mxcC	2,3-Dihydro-2,3-DHBA dehydrogenase	50	96	50	95
mxcL	Aldehyde aminotransferase	58	93	62	93
mxcM	Cytosine deaminase	—	—	—	—
mxcN	Major facilitator superfamily transporter	—	—	—	—
mxcO	AraC-type regulator	—	—	—	—
mxcP	TonB-dependent receptor	—	—	—	—
mxcD	Isochorismate synthase	36	93	36	92

[a]Similarities at the amino acid level for the corresponding enzymes in *P. piscicida* S2040, *S. aurantiaca* Sg a15, and *M. xanthus* DK 1622 are indicated. Id, identical amino acids; Qc, query cover; —, no homolog detected.

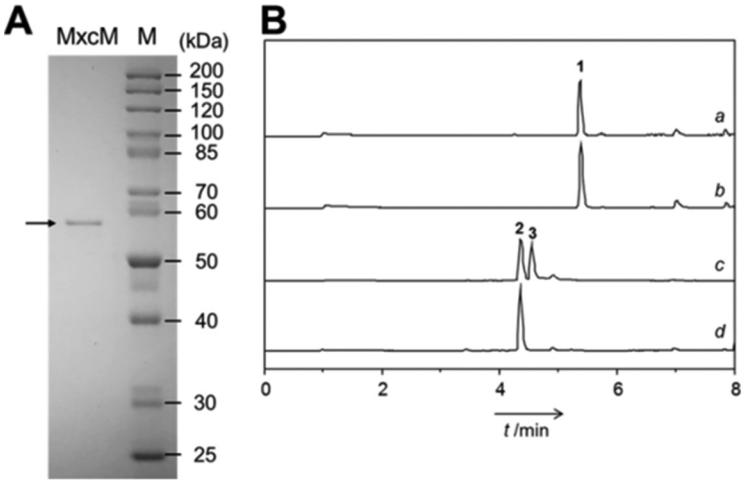

FIG 3 (A) SDS-PAGE of purified 6×His-MxcM. The calculated molecular mass of the recombinant protein is 58.786 kDa. Lane M, protein ladder. (B) Results of the *in vitro* testing of 6×His-MxcM. Total ion chromatograms of myxochelin A (compound 1) with 6×His-MxcM (profile *a*), myxochelin A (compound 1) without 6×His-MxcM (profile *b*), myxochelin B (compound 2) with 6×His-MxcM (profile *c*), and myxochelin B (compound 2) without 6×His-MxcM (profile *d*) are shown. The additional peak in profile *c* corresponds to pseudochelin A (compound 3).

mxcO, and *mxcP*) are exclusively present in the regulon of *P. piscicida* S2040. The *mxcN* and *mxcP* open reading frames are predicted to be involved in siderophore transport and uptake, whereas *mxcO* encodes a regulator of the AraC family. Therefore, a role in the formation of pseudochelin is conceivable only for *mxcM*, the product of which was annotated as cytosine deaminase (22).

Bioinformatic analysis of MxcM. A sequence analysis revealed that MxcM belongs to the amidohydrolase superfamily, whose members usually catalyze metal-dependent hydrolysis reactions (23, 24). One representative of this enzyme family, the imidazolonepropionase HutI, is known to cleave an imidazoline ring during histidine degradation (25). The reverse reaction, an intramolecular condensation, is reminiscent of the assumed formation of pseudochelin A. While sequence alignments of MxcM with different HutI homologs did not indicate significant similarities (see Table S1 in the supplemental material), a manual inspection showed that the active site residues of HutI (26, 27) are conserved in MxcM (Fig. S1A). However, the E252 residue of HutI, which seems necessary to initiate the hydrolysis reaction (26, 28), is replaced by a proline residue in MxcM. The closest homolog of MxcM with an assigned function is the amidohydrolase CbxE from *Streptomyces* sp. strain NTK937 (Fig. S1B and Table S2). This enzyme was found to be crucially involved in the biosynthesis of the benzoxazole antibiotic caboxamycin, and it was proposed to catalyze a two-step intramolecular cyclization and dehydration reaction, leading to the formation of an oxazoline ring (29). It is evident that the mechanism of this biosynthetic conversion is analogous to the formation of the imidazoline ring in pseudochelin A.

***In vitro* characterization of MxcM.** To verify the role of MxcM in pseudochelin A biosynthesis, the candidate gene was synthesized, cloned into pET28a, and overexpressed in *Escherichia coli* BL21(DE3) for the production of a 6×His-tagged protein. This recombinant enzyme was purified to homogeneity by immobilized metal affinity chromatography and was subsequently assayed with fermentation-derived myxochelin B (Fig. 3). High-performance liquid chromatography (HPLC) analysis showed the emergence of a new peak in the enzyme reaction, for which the high-resolution mass spectrometry (MS) and tandem mass spectrometry (MS/MS) data were consistent with pseudochelin A (21). When myxochelin B was incubated without 6×His-MxcM, no further peak was detected. Furthermore, the testing of synthetic myxochelin A (30) with 6×His-MxcM did not provide any evidence for an enzymatic conversion (Fig. 3).

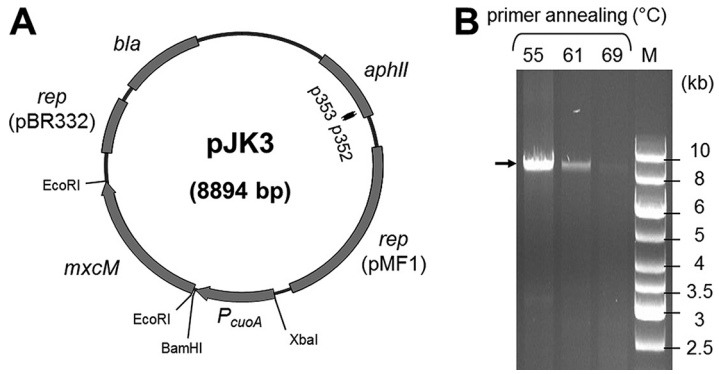

FIG 4 (A) Schematic map of the expression plasmid pJK3. Binding sites and the orientation of primers p352 and p353 are displayed as black arrows. (B) PCR-based confirmation of pJK3. A gradient PCR using biomass from the *M. xanthus* expression strain as the template was performed in order to amplify pJK3 with primers p352 and p353. The expected amplicon is marked with an arrow. Lane M, DNA ladder.

Construction of a vector for inducible expression of *mxcM* in *M. xanthus*. To demonstrate the functionality of MxcM under *in vivo* conditions, the corresponding gene was expressed in *M. xanthus* DSM 16526. This myxobacterial strain had been confirmed previously to synthesize myxochelin B and showed no signs of pseudochelin A production. For the gene transfer, a replicative expression plasmid was created. The respective vector was derived from pZJY156, which had been demonstrated to replicate stably in *M. xanthus* as well as in *E. coli* (31, 32). A codon-optimized version of the target gene *mxcM* from *P. piscicida* S2040 was cloned into the vector and placed under the control of the copper-inducible promoter P_{cuoA}. The expression of this promoter is known to correlate linearly with the copper concentration in the culture medium (33, 34). The final expression vector, pJK3 (Fig. 4A), was introduced into *M. xanthus* DSM 16526 via electroporation (35, 36). Transformants were selected by their acquired kanamycin resistance and, after several rounds of subcultivation, were analyzed by colony PCR to validate the presence of free, nonintegrated plasmid. The annealing sites of the primers used were located adjacent to each other inside the kanamycin resistance gene, thus leading to amplification of the entire pJK3 plasmid. Separation of the PCR products by horizontal electrophoresis revealed the expected product size of 8.9 kb (Fig. 4B). If any vector linearization had occurred (e.g., by integration of pJK3 into the host genome), then no PCR products would have been obtained. Ultimate evidence for the existence of autonomous plasmid DNA was obtained by sequencing (see Table S3 in the supplemental material).

Copper-induced expression of the *mxcM* gene in *M. xanthus* DSM 16526. Prior to the expression experiment, we evaluated the effect of the inducing agent ($CuSO_4$) on myxochelin production in the *M. xanthus* DSM 16526 wild-type strain. Since the liquid chromatography (LC)-MS profiles of supplemented and nonsupplemented cultures showed no differences, an impact of $CuSO_4$ on myxochelin production could be ruled out. Furthermore, it was verified that myxochelin production was not affected in an *M. xanthus* DSM 16526 strain carrying the empty expression vector (data not shown). Comparison of the extracts of wild-type and expression strains, after induction with 115 μM $CuSO_4$, by LC-MS measurements combined with MS/MS analyses indicated the presence of pseudochelin A exclusively in the extract of the expression strain (Fig. 5). MS/MS spectra of the putative pseudochelin A peak and an authentic myxochelin A standard both showed a Δ136 fragment (myxochelin A, *m/z* 405 → *m/z* 269; pseudochelin A, *m/z* 386 → *m/z* 250), which can be attributed to the loss of a 2,3-dihydroxybenzaldehyde moiety. The elimination of a 2,3-dihydroxybenzamide moiety was also observed (pseudochelin A, *m/z* 386 → *m/z* 233). These observations are in accordance with previous reports (21, 37). A distinctive Δ18 fragment of myxochelin A arises from the dehydration of its primary alcohol function in the lysinol residue. The

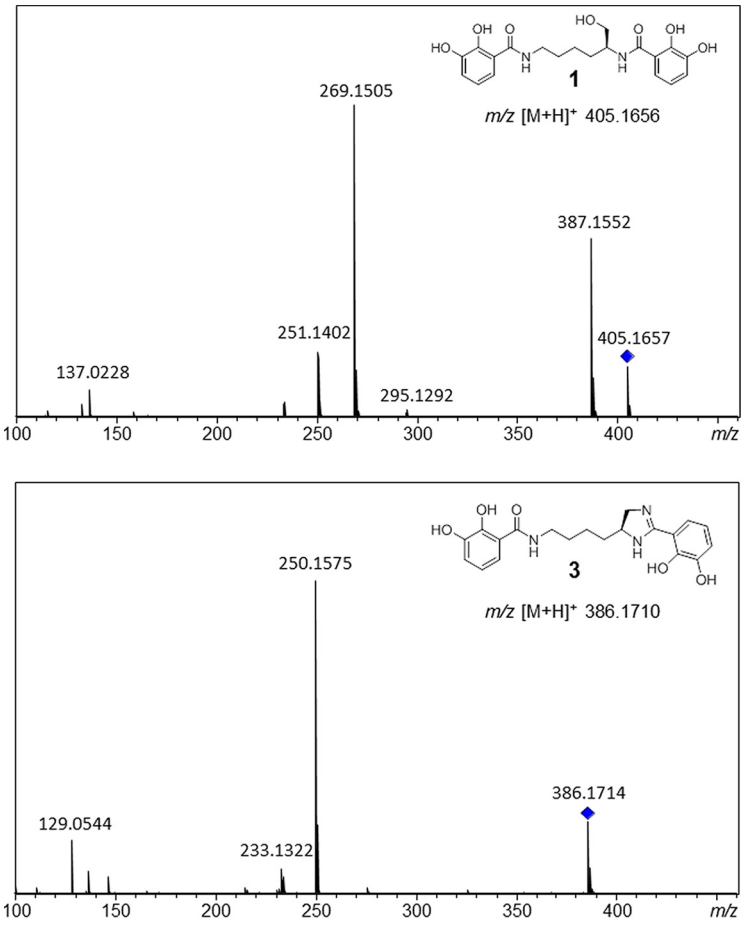

FIG 5 MS/MS fragmentation patterns of myxochelin A (compound 1) and pseudochelin A (compound 3). Parent ions are indicated with diamonds.

same structural motif is not present in pseudochelin A, which supports the MS-based assignment.

Constitutive expression of the *mxcM* gene in *M. xanthus* DSM 16526. To obtain unequivocal evidence that the *mxcM* gene is involved in the biosynthesis of pseudochelin A, we set out to confirm the identity of the heterologously produced compound by nuclear magnetic resonance (NMR) spectroscopy. However, only trace amounts of pseudochelin A could be recovered from the copper-inducible expression strain (data not shown). To evaluate whether the low production level could be overcome, P_{cuoA} was replaced with the constitutive promoter P_{pilA} (38), resulting in the generation of the expression vector pJK5 (Fig. S2). Transformation of *M. xanthus* DSM 16526 with this plasmid led to a strain exhibiting increased pseudochelin A titers. A total of 95 mg of pseudochelin A could be isolated from a 6-liter culture. NMR spectroscopic analyses of this material verified the identity of pseudochelin A (Fig. S3 to S7).

DISCUSSION

Pseudochelin A is a catechol siderophore that is structurally closely related to the myxochelins (10, 13) and hyalachelins (14). In this study, we identified a gene cluster for pseudochelin A biosynthesis in *P. piscicida* S2040 and we demonstrated that a single enzyme, MxcM, is needed to provide a myxochelin-producing bacterium the potential for pseudochelin biosynthesis.

From a biological perspective, the chemical diversity of myxochelin-type siderophores is intriguing. To date, however, it is unclear whether the minor structural differences between these compounds have important consequences, e.g., in terms

of iron affinity or siderophore uptake. Biosynthetic genes for the production of myxochelin-type molecules are found in several bacterial lineages, according to an analysis of genomic data. The occurrence of siderophore pathways in taxonomically distinct bacteria is not without precedence, as exemplified by the yersiniabactin locus (39). This wide distribution is usually attributed to lateral gene transfer and a strong evolutionary driving force to maintain the newly acquired biosynthesis genes (39). As expected, myxobacteria predominate among the myxochelin producers (see Fig. S8 in the supplemental material). The myxobacterial producer strains were isolated from different locations around the globe, which suggests that myxochelin biosynthesis arose quite early in this bacterial group. In contrast, very few actinomycetes were identified as myxochelin producers. Since myxobacteria and actinomycetes are both soil-inhabiting microorganisms, it is possible that some actinomycetes acquired the myxochelin biosynthesis genes by horizontal gene transfer. This would explain the restricted occurrence of the myxochelin regulon in this taxon.

Most myxobacteria that were analyzed possess the *mxcL* gene, but they lack an imidazoline synthase gene. Therefore, they are assumed to synthesize myxochelin B. Few bacteria (including 4 myxobacterial strains) were predicted to produce myxochelin A exclusively. The capacity for pseudochelin formation, specified by the presence of the amidohydrolase-encoding gene *mxcM*, seems to be restricted to members of the *Gammaproteobacteria*, particularly to members of the orders *Alteromonadales*, *Oceanospirillales*, and *Vibrionales* (Fig. S8). Considering the marine origin of the corresponding species (21, 40–43), the production of pseudochelin, compared to the myxochelins, might have an ecological advantage in aqueous environments. It is noteworthy in this context that the genomes of marine myxobacteria (44) are devoid of myxochelin biosynthesis genes.

Interestingly, homologs of MxcM are encoded not only in myxochelin-type pathways. The amidohydrolase CbxE from *Streptomyces* sp. strain NTK937 is involved in the biosynthesis of the antibiotic caboxamycin (29). While CbxE catalyzes the formation of an oxazoline ring, MxcM is responsible for imidazoline ring formation, putatively following an analogous reaction mechanism. Another homolog of MxcM was found in *Streptomyces megasporus* strain NRRL B-16372 (NCBI Protein accession number WP_031508998). The corresponding open reading frame is embedded in a gene cluster bearing remarkable similarity to the loci for antibiotic A33853 (45, 46) and nataxazole (47, 48) biosynthesis, which are found in the genomes of *Streptomyces* sp. strain NRRL 12068 and *Streptomyces* sp. strain Tü 6176, respectively.

In this study, the function of MxcM was probed *in vitro* as well as *in vivo* by heterologous expression in *M. xanthus*. This myxobacterium not only is a model organism for the analysis of bacterial motility, development, and predation (6, 49, 50) but also represents an attractive host for the reconstitution of biosynthetic pathways and genes. Of particular note in this context is its inherent proficiency in natural product assembly, including the allocation of a variety of biosynthetic building blocks (51). Although these properties are common to many fruiting myxobacteria, *M. xanthus* is further distinguished by its comparatively short generation time (52, 53) and its susceptibility to genetic manipulations (35, 36). Therefore, it is no surprise that *M. xanthus* has already served as host for the production of several secondary metabolites, including the myxobacterial compounds epothilone (53), myxothiazol (54), myxochromid (55), myxopyronin (56), corallopyronin (56), and vioprolide (57) and the actinobacterial polyketide oxytetracycline from *Streptomyces rimosus* (58). Hitherto, chromosomal integration of target genes was considered the method of choice for the engineering of *M. xanthus* expression strains. To this end, selected genes or entire biosynthetic gene clusters were incorporated into the chromosome, either by targeted homologous recombination or by random transpositional integration (53–58). The discovery of the first myxobacterial plasmid, pMF1, and the subsequent availability of a stable shuttle vector (31) set the stage for a plasmid-based expression system applicable in *M. xanthus*. Until now, however, pZJY156-derived vectors were utilized only during complementation studies, in order to restore certain gene functions in null mutants (31, 59).

In contrast to chromosomal integration, multicopy plasmids in general favor higher expression rates, due to manifold availability of the gene sequence. Therefore, it was expected that the pJK3-based expression of *mxcM* in *M. xanthus* would provide sufficient protein for the conversion of myxochelin B to pseudochelin A, especially since the wild-type strain had been identified as an efficient producer of myxochelin B. Nevertheless, only traces of pseudochelin A were detected in the corresponding strain. To test whether the copper-inducible expression affected the production of pseudochelin A, a promoter exchange was carried out. The resulting pJK5 strain, in which *mxcM* was constitutively expressed under the control of the P_{pilA} promoter, produced appreciable quantities of pseudochelin A. A possible explanation for the low productivity of the pJK3 strain might be that the expression of *mxcM* started too late. In that case, most of the biosynthesized myxochelin B would already have been secreted and the enzymatic conversion would have suffered from a lack of substrate in the myxobacterial cells. Although the tight copper dependency and functionality of the P_{cuoA} promoter had been demonstrated previously in *M. xanthus*, it had also been noted that the promoter reached its greatest activity 24 to 48 h after copper addition (34). The delayed response of the P_{cuoA} promoter and consequently the delayed formation of active enzyme inside the host, combined with the active efflux of the siderophore, would also provide an explanation for the observed accumulation of myxochelin B in the culture broth of the pJK3 strain.

In summary, the previously proposed enzymatic conversion of myxochelin B into pseudochelin A could be verified, and the amidohydrolase involved, MxcM, was identified. Furthermore, heterologous production of pseudochelin A in the nonnative host *M. xanthus* was achieved using a plasmid-based expression system. The capacity for myxochelin biosynthesis was shown to be much more widespread than reported previously, and pseudochelin A biosynthesis could be traced back uniquely to members of *Gammaproteobacteria*.

MATERIALS AND METHODS

Strains and growth conditions. *M. xanthus* DSM 16526 wild-type and expression strains were routinely cultured in modified CTPM medium (1.0% [wt/vol] casitone, 0.12% [wt/vol] Tris, 0.02% [wt/vol] KH_2PO_4, 0.06% [wt/vol] $MgSO_4 \cdot 7H_2O$, and 0.00005% [wt/vol] vitamin B_{12} [pH 7.5]) (60). Cultivation was conducted at 30°C, and liquid cultures were shaken at 130 rpm. *Escherichia coli* DH5α and *E. coli* BL21(DE3) were grown in standard lysogeny broth (LB) (Carl Roth) at 37°C, with agitation at 200 rpm. Antibiotics were used, when necessary, at the following concentrations: 100 μg/ml ampicillin, and 50 μg/ml kanamycin.

Analytical methods. HPLC experiments were conducted with a Shimadzu HPLC system (LC-20AD system with SPD-M20A detector). LC-MS and LC-MS/MS analyses were performed with an Agilent 1260 Infinity HPLC system combined with a Compact quadrupole-time of flight (Q-TOF) mass spectrometer (Bruker Daltonics). The Q-TOF mass spectrometer was interfaced with an electrospray ionization source. All analyses were performed in positive ion mode using a capillary potential of 4.5 kV. The desolvation gas (N_2) temperature was 220°C, with a flow rate of 12 liters/min. Compounds were infused into the electrospray source by the 1260 Infinity HPLC system at a flow rate of 0.4 ml/min. The protonated molecular ions of test compounds were generated at an end plate offset of 500 V. Nitrogen was used as the collision gas, at a pressure of 5 mPa. MS/MS experiments were performed in multiple reaction monitoring (MRM) mode, with a collision gas energy of 23 eV. NMR spectra were recorded on a Bruker AV 600-MHz Avance III HD system (CryoProbe), with methanol-d_4 as the solvent and internal standard. The solvent signals were referenced to δ_H 3.31 ppm and δ_C 49.0 ppm.

Production and purification of myxochelin B. For the production of myxochelin B, *M. xanthus* DSM 16526 was grown for 5 days in modified CTPM medium supplemented with DHBA. The biosynthetic precursor was added as a filter-sterilized solution (final concentration, 30 mg/liter) prior to the inoculation of *M. xanthus*. To facilitate the recovery of the siderophore, the myxobacteria were grown in the presence of 2% (wt/vol) Amberlite XAD7HP resin (Sigma-Aldrich). At the end of cultivation, the adsorber resin was collected by filtration, washed with water, and extracted exhaustively with methanol. Isolation of myxochelin B from the methanol extract was accomplished with two consecutive reverse-phase HPLC steps. The initial separation was carried out on a Nucleodur C_{18} gravity column (250 by 10 mm, 3 μm; Macherey-Nagel), using a linear gradient of methanol in water supplemented with 0.1% (vol/vol) trifluoroacetic acid (10% to 100% methanol within 15 min, followed by 100% methanol for an additional 10 min), at a flow rate of 2.5 ml/min. Final purification of myxochelin B was achieved on a Nucleodur Sphinx RP column (250 by 10 mm, 5 μm; Macherey-Nagel), with identical eluents and flow rate but a different gradient (25% to 48% methanol over 27 min, 48% to 75% methanol within 8 min, and 75% methanol for 5 min). The elution of compounds was monitored with a diode array detector.

TABLE 2 Plasmids used in this study

Plasmid	Relevant properties[a]	Source or reference
pET28a(+)	*E. coli* expression vector; Km^r	Novagen
pET28a(+)-*mxcM*	pET28a(+) carrying synthetic *mxcM* gene; Km^r	This study
pJET1.2	*E. coli* cloning vector; Amp^r	Thermo Fisher Scientific
pJK1	pJET1.2 carrying 825-bp promoter region P_{cuoA} from DSM 16526; Amp^r	This study
pJK2	Subcloning vector, pZJY156-*mxcM*; Km^r	This study
pJK3	*M. xanthus* expression vector, pZJY156-P_{cuoA}-*mxcM*; Km^r	This study
pJK4	pJET1.2 carrying 207-bp promoter region P_{pilA} from DSM 16526; Amp^r	This study
pJK5	*M. xanthus* expression vector, pZJY156-P_{pilA}-*mxcM*; Km^r	This study
pZJY156	*M. xanthus-E. coli* shuttle vector; Amp^r, Km^r	31, 32

[a]Km^r, kanamycin resistance; Amp^r, ampicillin resistance.

Plasmids, nucleic acids, and protein sequences. Plasmids used in this study are listed in Table 2. The native *mxcM* gene can be found in GenBank under the locus tag TW75_RS20450 (GenBank protein accession number WP_045965770). The shuttle vector pZJY156 and the codon-adapted version of the *P. piscicida mxcM* gene were synthesized by ATG:biosynthetics. The codon adaptation of *mxcM* was carried out manually, referring to the codon usage of *M. xanthus* deposited in the Kazusa database (61). Nucleotide sequences of *P. piscicida* S2040, *Stigmatella aurantiaca* Sg a15, and *Myxococcus xanthus* DK 1622 were retrieved from GenBank (accession numbers NZ_JXXW00000000, AF299336, and NC_008095, respectively). Homologies of nucleotide sequences were evaluated using the Basic Local Alignment Search Tool (BLAST) (62). Protein sequences of imidazolonepropionases were also obtained from GenBank. Alignments were performed with the open access software GeneStudio Pro.

General DNA methods. Genomic DNA was extracted from *M. xanthus* DSM 16526 following a previously published protocol (63). Plasmids from *E. coli* DH5α were isolated using a Roti-Prep plasmid minikit (Carl Roth). DNA fragments from agarose electrophoresis gels were extracted with the QIAquick gel extraction kit (Qiagen). Restriction digestions were performed using FastDigest restriction enzymes (Thermo Fisher Scientific). Ligation of DNA fragments was achieved using a T4 DNA ligase (Thermo Fisher Scientific). If required, plasmid DNA was dephosphorylated, using the FastAP thermosensitive alkaline phosphatase (Thermo Fisher Scientific), prior to ligation. Subcloning was performed in *E. coli* DH5α using standard protocols.

Production and purification of recombinant 6×His-MxcM. The synthetic *mxcM* gene was cloned into the EcoRI restriction site of pET28a(+). The resulting expression plasmid, pET28a(+)-*mxcM*, was transferred into chemically competent *E. coli* BL21(DE3). For the production of 6×His-tagged MxcM, the expression strain was cultivated at 37°C in terrific broth medium (12.0% [wt/vol] tryptone/peptone, 24.0% [wt/vol] yeast extract, 0.4% [vol/vol] glycerol, 2.3% [wt/vol] KH_2PO_4, and 12.5% [wt/vol] K_2HPO_4), to an optical density at 600 nm (OD_{600}) of 0.6. After induction with isopropyl-β-D-1-thiogalactopyranoside (IPTG) (final concentration, 1 mM), the incubation was continued at 16°C for 20 h. Cells were harvested by centrifugation (4,000 rpm for 15 min at 4°C) and resuspended in lysis buffer (50 mM NaH_2PO_4 [pH 8.0], 10 mM imidazole, 300 mM NaCl, and 10% glycerol). After cell disruption by ultrasonic treatment, the cell debris was removed by centrifugation (4,500 rpm for 30 min at 4°C). Purification of 6×His-labeled MxcM from the supernatant was achieved by affinity chromatography using Protino Ni-nitrilotriacetic acid (NTA)-agarose (Macherey-Nagel) as the stationary phase, in a polypropylene column (Qiagen). The recombinant protein was eluted using lysis buffer containing 250 mM imidazole. After desalting with a PD-10 desalting column (GE Healthcare Life Sciences) and concentration with an Amicon centrifugal filter unit (Ultra-15, with a molecular weight cutoff value of 10 kDa; Merck Millipore), 6×His-MxcM was kept in 0.1 M phosphate buffer (pH 7.0).

***In vitro* testing of 6×His-MxcM.** Hexahistidine-tagged MxcM (final concentration, 2 μM) was incubated at 30°C with myxochelin A or B (0.5 mM) and 50 mM Tris-HCl buffer (pH 7.0), in a total reaction volume of 0.5 ml. As controls, the substrate and/or the recombinant enzyme was omitted. After 1 h, the reaction was stopped by the addition of 15% (vol/vol) acetonitrile. Product formation was analyzed by LC-MS measurements.

Construction of the myxobacterial expression vectors pJK3 and pJK5. The promoter regions P_{cuoA} and P_{pilA} were amplified from *M. xanthus* DSM 16526 genomic DNA using the Phusion Flash high-fidelity PCR master mix (Thermo Fisher Scientific). The primers p357 (5′-GCATGGATCCGAAGCCTC TTCACGAATGGATGG-3′) and p358 (5′-GAGCTCTAGATGTCGGCCATGAACGGCACTTCACG-3′), carrying BamHI and XbaI restriction sites, respectively, were used to amplify the region 825 bp upstream of the *cuoA* gene (locus tag MXAN_3420). The PCR was conducted with the following conditions: 98°C for 10 s; 30 cycles of 98°C for 1 s, 64°C for 5 s, and 72°C for 12 s; and 72°C for 1 min. The amplicon was ligated into pJET1.2 to yield pJK1. Subsequently, the synthetic gene *mxcM*, in its codon-adapted form, was ligated into the EcoRI site of pZJY156 in order to create pJK2. The P_{cuoA} sequence was excised from pJK1 using BamHI and XbaI. The vector pJK2 was also digested with BamHI and XbaI and the backbone fragment was ligated with the promoter sequence to generate the expression vector pJK3. To amplify the region 207 bp upstream of the *pilA* gene (locus tag MXAN_5783), we used the primers p493 (5′-GGAT CCGGGAGCGCTTCGGATGCGTAG-3′) and p494 (5′-GGTACCGGGGGTCCTCAGAGAAGG-3′), which introduced BamHI and KpnI restriction sites into the PCR product. The PCR was conducted as described before. The resulting amplicon was subcloned into pJET1.2 to yield pJK4; after digestion, the corresponding DNA fragment was ligated into the BamHI-KpnI site of pJK2 to generate the expression vector pJK5.

Generation of the *M. xanthus* expression strains. Transformation of *M. xanthus* DSM 16526 was achieved by electroporation, according to previously published protocols (35, 36). To verify the successful uptake of the plasmids pJK3 and pJK5, the *M. xanthus* transformants were grown for 4 to 5 days at 30°C on solid CTPM medium supplemented with kanamycin. Biomass was collected and used as the template for colony PCR. For this purpose, cells were suspended in MilliQ water and incubated for 3 min at 99°C. The PCR was performed using DreamTaq DNA polymerase (Thermo Fisher Scientific). The optimum primer annealing was examined using a temperature gradient from 55°C to 69°C. The PCR was conducted under the following conditions: 95°C for 3 min; 30 cycles of 95°C for 45 s, 55°C/61°C/69°C for 30 s, and 72°C for 8 min; and final extension at 72°C for 10 min. Primers p352 (5′-GCTGACCGCTTCCTCGTGCTTTACG-3′) and p353 (5′-CCGCCAAGCTCTTCAGCAATATCACGGG-3′) were used in order to amplify the entire pJK3 (size, 8.9 kb) or pJK5 (size, 8.3 kb) plasmid. The corresponding PCR products were purified and used as the templates for subsequent PCRs in order to amplify the kanamycin resistance gene *aphII* with primers p268 (5′-GGATTGCACGCAGGTTCTCCGG-3′) and p269 (5′-CGATAGAAGGCGATGCGCTGCG-3′) and the pMF1-based origin of replication with primers p342 (5′-CTGGTGCCTGTCGTCATGGAGAC-3′) and p343 (5′-CACGCACACCGACGAGTCATAG-3′). The pBR332-based origin of replication was amplified together with the ampicillin resistance gene *bla* using the primers p344 (5′-GCTCAAGTCAGAGGTGGCGAAACC-3′) and p345 (5′-GCGAGACGAAAGGGCCTCGTGATACGCC-3′). The PCR products were purified and used as the templates for sequencing reactions (Microsynth Seqlab).

Heterologous production and isolation of pseudochelin A from recombinant *M. xanthus*. In order to maintain the pJK3 and pJK5 vectors, cultures of the *M. xanthus* expression strains were grown in the presence of kanamycin. Expression of the target gene in pJK3 was induced by the addition of copper(II) sulfate (115 μM). After 4 days of incubation, the culture broths were extracted with ethyl acetate, and pseudochelin A production was verified by high-resolution MS and MS/MS analyses. Myxochelin A served as a control during these experiments. For the isolation of pseudochelin A, the *M. xanthus* strain harboring pJK5 was incubated for 4 days in modified CTPM medium supplemented with 2,3-DHBA. To assist recovery of the metabolite, cultivation was carried out in the presence of 2% (wt/vol) Amberlite XAD7HP resin (Sigma-Aldrich). At the end of fermentation, the adsorber resin was collected by filtration, washed with water, and exhaustively eluted with methanol. Isolation of pseudochelin A from the methanol extract was accomplished by two consecutive reverse-phase HPLC steps. The first separation was achieved on a Nucleodur 100-5 C_{18} ec VarioPrep column (125 by 21 mm, 5 μm; Macherey-Nagel), using a linear gradient of methanol in water supplemented with 0.1% (vol/vol) trifluoroacetic acid (15% to 60% methanol within 20 min, 60% to 100% over 5 min, and 100% methanol for an additional 7 min), at a flow rate of 8 ml/min. Final purification of pseudochelin A was achieved on the same column with identical eluents and flow rate but under isocratic conditions, using a mobile phase consisting of 32% methanol. The elution of compounds was monitored with a diode array detector.

Accession number(s). The nucleotide sequence of the synthetic *mxcM* gene was deposited in GenBank under accession number MH248775.

SUPPLEMENTAL MATERIAL

Supplemental material for this article may be found at https://doi.org/10.1128/AEM.01789-18.

SUPPLEMENTAL FILE 1, PDF file, 1.1 MB.

ACKNOWLEDGMENTS

Financial support from the Bundesministerium für Bildung und Forschung within the program InfectControl 2020 (grant 03ZZ0808A) is gratefully acknowledged.

We thank Anna Tippelt for valuable discussions and Katharina Kuhr and Chantale Zammarelli (TU Dortmund University) for conducting MS and MS/MS measurements. We thank Karin Martin and Florian Baldeweg (Leibniz Institute for Natural Product Research and Infection Biology) for technical support.

REFERENCES

1. Andrews SC, Robinson AK, Rodríguez-Quiñones F. 2003. Bacterial iron homeostasis. FEMS Microbiol Rev 27:215–237. https://doi.org/10.1016/S0168-6445(03)00055-X.
2. Saha R, Saha N, Donofrio RS, Bestervelt LL. 2013. Microbial siderophores: a mini review. J Basic Microbiol 53:303–317. https://doi.org/10.1002/jobm.201100552.
3. Kurth C, Kage H, Nett M. 2016. Siderophores as molecular tools in medical and environmental applications. Org Biomol Chem 14:8212–8227. https://doi.org/10.1039/C6OB01400C.
4. Velicer GJ, Vos M. 2009. Sociobiology of the myxobacteria. Annu Rev Microbiol 63:599–623. https://doi.org/10.1146/annurev.micro.091208.073158.
5. Cao P, Dey A, Vassallo CN, Wall D. 2015. How myxobacteria cooperate. J Mol Biol 427:3709–3721. https://doi.org/10.1016/j.jmb.2015.07.022.
6. Bretl DJ, Kirby JR. 2016. Molecular mechanisms of signaling in *Myxococcus xanthus* development. J Mol Biol 428:3805–3830. https://doi.org/10.1016/j.jmb.2016.07.008.
7. Schäberle TF, Lohr F, Schmitz A, König GM. 2014. Antibiotics from myxobacteria. Nat Prod Rep 31:953–972. https://doi.org/10.1039/c4np00011k.
8. Korp J, Vela Gurovic MS, Nett M. 2016. Antibiotics from predatory bacteria. Beilstein J Org Chem 12:594–607. https://doi.org/10.3762/bjoc.12.58.
9. Herrmann J, Fayad AA, Müller R. 2017. Natural products from myxobacteria: novel metabolites and bioactivities. Nat Prod Rep 34:135–160. https://doi.org/10.1039/C6NP00106H.
10. Kunze B, Bedorf N, Kohl W, Höfle G, Reichenbach H. 1989. Myxochelin A, a new iron-chelating compound from *Angiococcus disciformis*

(Myxobacterales): production, isolation, physico-chemical and biological properties. J Antibiot (Tokyo) 42:14–17. https://doi.org/10.7164/antibiotics.42.14.
11. Gaitatzis N, Kunze B, Müller R. 2005. Novel insights into siderophore formation in myxobacteria. ChemBioChem 6:365–374. https://doi.org/10.1002/cbic.200400206.
12. Krug D, Zurek G, Revermann O, Vos M, Velicer GJ, Müller R. 2008. Discovering the hidden secondary metabolome of *Myxococcus xanthus*: a study of intraspecific diversity. Appl Environ Microbiol 74:3058–3068. https://doi.org/10.1128/AEM.02863-07.
13. Schieferdecker S, König S, Koeberle A, Dahse HM, Werz O, Nett M. 2015. Myxochelins target human 5-lipoxygenase. J Nat Prod 78:335–338. https://doi.org/10.1021/np500909b.
14. Nadmid S, Plaza A, Lauro G, Garcia R, Bifulco G, Müller R. 2014. Hyalachelins A–C, unusual siderophores isolated from the terrestrial myxobacterium *Hyalangium minutum*. Org Lett 16:4130–4133. https://doi.org/10.1021/ol501826a.
15. Miyanaga S, Obata T, Onaka H, Fujita T, Saito N, Sakurai H, Saiki I, Furumai T, Igarashi Y. 2006. Absolute configuration and antitumor activity of myxochelin A produced by *Nonomuraea pusilla* TP-A0861. J Antibiot (Tokyo) 59:698–703. https://doi.org/10.1038/ja.2006.93.
16. Kiss H, Nett M, Domin N, Martin K, Maresca JA, Copeland A, Lapidus A, Lucas S, Berry KW, Glavina Del Rio T, Dalin E, Tice H, Pitluck S, Richardson P, Bruce D, Goodwin L, Han C, Detter JC, Schmutz J, Brettin T, Land M, Hauser L, Kyrpides NC, Ivanova N, Göker M, Woyke T, Klenk HP, Bryant DA. 2011. Complete genome sequence of the filamentous gliding predatory bacterium *Herpetosiphon aurantiacus* type strain (114-95^T). Stand Genomic Sci 5:356–370. https://doi.org/10.4056/sigs.2194987.
17. Silakowski B, Kunze B, Nordsiek G, Blöcker H, Höfle G, Müller R. 2000. The myxochelin iron transport regulon of the myxobacterium *Stigmatella aurantiaca* Sg a15. Eur J Biochem 267:6476–6485. https://doi.org/10.1046/j.1432-1327.2000.01740.x.
18. Gaitatzis N, Kunze B, Müller R. 2001. *In vitro* reconstitution of the myxochelin biosynthesis machinery of *Stigmatella aurantiaca* Sg a15: biochemical characterization of a reductive release mechanism from nonribosomal peptide synthetases. Proc Natl Acad Sci U S A 98:11136–11141. https://doi.org/10.1073/pnas.201167098.
19. Li Y, Weissman KJ, Müller R. 2008. Myxochelin biosynthesis: direct evidence for two- and four-electron reduction of a carrier protein-bound thioester. J Am Chem Soc 130:7554–7555. https://doi.org/10.1021/ja8025278.
20. Korp J, König S, Schieferdecker S, Dahse H-M, König GM, Werz O, Nett M. 2015. Harnessing enzymatic promiscuity in myxochelin biosynthesis for the production of 5-lipoxygenase inhibitors. ChemBioChem 16:2445–2450. https://doi.org/10.1002/cbic.201500446.
21. Sonnenschein EC, Stierhof M, Goralczyk S, Vabre FM, Pellissier L, Hanssen KØ, de la Cruz M, Díaz C, de Witte P, Copmans D, Andersen JH, Hansen E, Kristoffersen V, Tormo JR, Ebel R, Milne BF, Deng H, Gram L, Jaspars M, Tabudravu JN. 2017. Pseudochelin A, a siderophore of *Pseudoalteromonas piscicida* S2040. Tetrahedron 73:2633–2637. https://doi.org/10.1016/j.tet.2017.03.051.
22. Machado H, Sonnenschein EC, Melchiorsen J, Gram L. 2015. Genome mining reveals unlocked bioactive potential of marine Gram-negative bacteria. BMC Genomics 16:158. https://doi.org/10.1186/s12864-015-1365-z.
23. Holm H, Sander C. 1997. An evolutionary treasure: unification of a broad set of amidohydrolases related to urease. Proteins 28:72–82. https://doi.org/10.1002/(SICI)1097-0134(199705)28:1<72::AID-PROT7>3.0.CO;2-L.
24. Seibert CM, Raushel FM. 2005. Structural and catalytic diversity within the amidohydrolase superfamily. Biochemistry 44:6383–6391. https://doi.org/10.1021/bi047326v.
25. Michal G. 1999. Biochemical pathways: an atlas of biochemistry and molecular biology. John Wiley & Sons, New York, NY.
26. Yu Y, Liang YH, Brostromer E, Quan JM, Panjikar S, Dong YH, Su XD. 2006. A catalytic mechanism revealed by the crystal structures of the imidazolonepropionase from *Bacillus subtilis*. J Biol Chem 281:36929–36936. https://doi.org/10.1074/jbc.M607703200.
27. Tyagi R, Eswaramoorthy S, Burley SK, Raushel FM, Swaminathan S. 2008. A common catalytic mechanism for proteins of HutI family. Biochemistry 47:5608–5615. https://doi.org/10.1021/bi800180g.
28. Su H, Sheng X, Liu Y. 2016. Exploring the substrate specificity and catalytic mechanism of imidazolonepropionase (HutI) from *Bacillus subtilis*. Phys Chem Chem Phys 18:27928–27938. https://doi.org/10.1039/C6CP04918D.
29. Losada AA, Cano-Prieto C, García-Salcedo R, Braña AF, Méndez C, Salas JA, Olano C. 2017. Caboxamycin biosynthesis pathway and identification of novel benzoxazoles produced by cross-talk in *Streptomyces* sp. NTK 937. Microb Biotechnol 10:873–885. https://doi.org/10.1111/1751-7915.12716.
30. Schieferdecker S, Nett M. 2016. A fast and efficient method for the preparation of the 5-lipoxygenase inhibitor myxochelin A. Tetrahedron Lett 57:1359–1360. https://doi.org/10.1016/j.tetlet.2016.02.047.
31. Zhao JY, Zhong L, Shen MJ, Xia ZJ, Cheng QX, Sun X, Zhao GP, Li YZ, Qin ZJ. 2008. Discovery of the autonomously replicating plasmid pMF1 from *Myxococcus fulvus* and development of a gene cloning system in *Myxococcus xanthus*. Appl Environ Microbiol 74:1980–1987. https://doi.org/10.1128/AEM.02143-07.
32. Feng J, Chen XJ, Sun X, Wang N, Li YZ. 2012. Characterization of the replication origin of the myxobacterial self-replicative plasmid pMF1. Plasmid 68:105–112. https://doi.org/10.1016/j.plasmid.2012.04.001.
33. Sánchez-Sutil MC, Gómez-Santos N, Moraleda-Muñoz A, Martins LO, Pérez J, Muñoz-Dorado J. 2007. Differential expression of the three multicopper oxidases from *Myxococcus xanthus*. J Bacteriol 189:4887–4898. https://doi.org/10.1128/JB.00309-07.
34. Gómez-Santos N, Treuner-Lange A, Moraleda-Muñoz A, García-Bravo E, García-Hernández R, Martínez-Cayuela M, Pérez J, Søgaard-Andersen L, Muñor-Dorado J. 2012. Comprehensive set of integrative plasmid vectors for copper-inducible gene expression in *Myxococcus xanthus*. Appl Environ Microbiol 78:2515–2521. https://doi.org/10.1128/AEM.07502-11.
35. Kashefi K, Hartzell PL. 1995. Genetic suppression and phenotypic masking of a *Myxococcus xanthus frzF*$^-$ defect. Mol Microbiol 15:483–494. https://doi.org/10.1111/j.1365-2958.1995.tb02262.x.
36. Youderian P, Burke N, White DJ, Hartzell PL. 2003. Identification of genes required for adventurous gliding motility in *Myxococcus xanthus* with the transposable element mariner. Mol Microbiol 49:555–570. https://doi.org/10.1046/j.1365-2958.2003.03582.x.
37. Kim J, Choi JN, Kim P, Sok DE, Nam SW, Lee CH. 2009. LC-MS/MS profiling-based secondary metabolite screening of *Myxococcus xanthus*. J Microbiol Biotechnol 19:51–54.
38. Wu SS, Kaiser D. 1997. Regulation of expression of the *pilA* gene in *Myxococcus xanthus*. J Bacteriol 179:7748–7758. https://doi.org/10.1128/jb.179.24.7748-7758.1997.
39. Greule A, Marolt M, Deubel D, Peintner I, Zhang S, Jessen-Trefzer C, De Ford C, Burschel S, Li S-M, Friedrich T, Merfort I, Lüdeke S, Bisel P, Müller M, Paululat T, Bechthold A. 2017. Wide distribution of foxicin biosynthetic gene clusters in *Streptomyces* strains: an unusual secondary metabolite with various properties. Front Microbiol 8:221. https://doi.org/10.3389/fmicb.2017.00221.
40. Holmström C, Kjelleberg S. 1999. Marine *Pseudoalteromonas* species are associated with higher organisms and produce biologically active extracellular agents. FEMS Microbiol Ecol 30:285–293. https://doi.org/10.1016/S0168-6496(99)00063-X.
41. Lee HK, Chun J, Moon EY, Ko SH, Lee DS, Lee HS, Bae KS. 2001. *Hahella chejuensis* gen. nov., sp. nov., an extracellular-polysaccharide-producing marine bacterium. Int J Syst Evol Microbiol 51:661–666. https://doi.org/10.1099/00207713-51-2-661.
42. Liu Y, Zhang Z, Wang Y, Zheng Y, Zhang XH. 2016. *Enterovibrio pacificus* sp. nov., isolated from seawater, and emended descriptions of *Enterovibrio coralii* and the genus *Enterovibrio*. Int J Syst Evol Microbiol 66:319–325. https://doi.org/10.1099/ijsem.0.000721.
43. Amin AKMR, Tanaka M, Al-Saari N, Feng G, Mino S, Ogura Y, Hayashi T, Meirelles PM, Thompson FL, Gomez-Gil B, Sawabe T, Sawabe T. 2017. *Thaumasiovibrio occultus* gen. nov. sp. nov. and *Thaumasiovibrio subtropicus* sp. nov. within the family *Vibrionaseae*, isolated from coral reed seawater off Ishigaki Island, Japan. Syst Appl Microbiol 40:290–296. https://doi.org/10.1016/j.syapm.2017.04.003.
44. Dávila-Céspedes A, Hufendiek P, Crüsemann M, Schäberle TF, König GM. 2016. Marine-derived myxobacteria of the suborder Nannocystineae: an underexplored source of structurally intriguing and biologically active metabolites. Beilstein J Org Chem 12:969–984. https://doi.org/10.3762/bjoc.12.96.
45. Michel KH, Boeck LD, Hoehn MM, Jones ND, Chaney MO. 1984. The discovery, fermentation, and structure of antibiotic A33853 and its tetraacetyl derivative. J Antibiot (Tokyo) 37:441–445. https://doi.org/10.7164/antibiotics.37.441.
46. Lv M, Zhao J, Deng Z, Yu Y. 2015. Characterization of the biosynthetic gene cluster of benzoxazole antibiotic A33853 reveals unusual assembly

logic. Chem Biol 22:1313–1324. https://doi.org/10.1016/j.chembiol.2015.09.005.
47. Sommer PS, Almeida RC, Schneider K, Beil W, Süssmuth RD, Fiedler HP. 2008. Nataxazole, a new benzoxazole derivative with antitumor activity produced by *Streptomyces* sp. Tü 6176. J Antibiot (Tokyo) 61:683–686. https://doi.org/10.1038/ja.2008.97.
48. Cano-Prieto C, García-Salcedo R, Sánchez-Hidalgo M, Braña AF, Fiedler HP, Méndez C, Salas JA, Olano C. 2015. Genome mining of *Streptomyces* sp. Tü 6176: characterization of the nataxazole biosynthetic pathway. ChemBioChem 16:1461–1473. https://doi.org/10.1002/cbic.201500153.
49. Zusman DR, Scott AE, Yang Z, Kirby JR. 2007. Chemosensory pathways, motility and development in *Myxococcus xanthus*. Nat Rev Microbiol 5:862–872. https://doi.org/10.1038/nrmicro1770.
50. Keane R, Berleman J. 2016. The predatory life cycle of *Myxococcus xanthus*. Microbiology 162:1–11. https://doi.org/10.1099/mic.0.000208.
51. Wenzel SC, Müller R. 2009. Myxobacteria: 'microbial factories' for the production of bioactive secondary bioactive secondary metabolites. Mol Biosyst 5:567–574. https://doi.org/10.1039/b901287g.
52. Dworkin M. 1962. Nutritional requirements for vegetative growth of *Myxococcus xanthus*. J Bacteriol 84:250–257.
53. Julien B, Shah S. 2002. Heterologous expression of epothilone biosynthetic genes in *Myxococcus xanthus*. Antimicrob Agents Chemother 46:2772–2778. https://doi.org/10.1128/AAC.46.9.2772-2778.2002.
54. Perlova O, Fu J, Kuhlmann S, Krug D, Stewart AF, Zhang Y, Müller R. 2006. Reconstitution of the myxothiazol biosynthetic gene cluster by Red/ET recombination and heterologous expression in *Myxococcus xanthus*. Appl Environ Microbiol 72:7485–7494. https://doi.org/10.1128/AEM.01503-06.
55. Fu J, Wenzel SC, Perlova O, Wang J, Gross F, Tang Z, Yin Y, Stewart AF, Müller R, Zhang Y. 2008. Efficient transfer of two large secondary metabolite pathway gene clusters into heterologous hosts by transposition. Nucleic Acids Res 36:e113. https://doi.org/10.1093/nar/gkn499.
56. Sucipto H, Pogorev D, Luxenberger E, Wenzel SC, Müller R. 2017. Heterologous production of myxobacterial α-pyrone antibiotics in *Myxococcus xanthus*. Metab Eng 44:160–170. https://doi.org/10.1016/j.ymben.2017.10.004.
57. Yan F, Auerbach D, Chai Y, Keller L, Tu Q, Hüttel S, Glemser A, Grab HA, Bach T, Zhang Y, Müller R. 2018. Biosynthesis and heterologous production of vioprolides: rational biosynthetic engineering and unprecedented 4-methylazetidine-carboxylic acid formation. Angew Chem Int Ed Engl 57:8754–8759. https://doi.org/10.1002/anie.201802479.
58. Stevens DC, Henry MR, Murphy KA, Boddy CN. 2010. Heterologous expression of the oxytetracycline biosynthetic pathway in *Myxococcus xanthus*. Appl Environ Microbiol 76:2681–2683. https://doi.org/10.1128/AEM.02841-09.
59. Bhat S, Zhu X, Patel RP, Orlando R, Shimkets LJ. 2011. Identification and localization of *Myxococcus xanthus* porins and lipoproteins. PLoS One 6:e27475. https://doi.org/10.1371/journal.pone.0027475.
60. Hartzell PL. 1997. Complementation of sporulation and motility defects in prokaryote by a eukaryotic GTPase. Proc Natl Acad Sci U S A 94:9881–9886.
61. Nakamura Y, Gojobori T, Ikemura T. 1997. Codon usage tabulated from the international DNA sequence databases. Nucleic Acids Res 25:244–245. https://doi.org/10.1093/nar/25.1.244.
62. Altschul SF, Gish W, Miller W, Myers EW, Lipman DJ. 1990. Basic local alignment search tool. J Mol Biol 215:403–410. https://doi.org/10.1016/S0022-2836(05)80360-2.
63. Neumann B, Pospiech A, Schairer HU. 1992. Rapid isolation of genomic DNA from Gram-negative bacteria. Trends Genet 8:332–333. https://doi.org/10.1016/0168-9525(92)90269-A.